

# $E_z$ -response as a monitor of a Baikal rift fault electrical resistivity: 3D modelling studies

Oleg V. Pankratov, Alexei V. Kuvshinov, Dmitry B. Avdeev, Vitaly S. Shneyer and Igor L. Trofimov  
*Geoelectromagnetic Research Institute, Russian Academy of Sciences, Moscow Region, Russia*

## Abstract

3D numerical studies have shown that the vertical voltage above the Baikal deep-water fault is detectable and that respective transfer functions,  $E_z$ -responses, are sensitive to the electrical resistivity changes of the fault, *i.e.* these functions appear actually informative with respect to the resistivity «breath» of the fault. It means that if the fault resistivity changed, conventional electromagnetic instruments would be able to detect this fact by measurement of the vertical electric field,  $E_z$ , or the vertical electric voltage just above the fault as well as horizontal magnetic field on the shore. Other electromagnetic field components ( $E_x$ ,  $E_y$ ,  $H_z$ ) do not seem to be sensitive to the resistivity changes in such a thin fault (as wide as 500 m). On the other hand, such changes are thought to be able to indicate a change of a stress state in the earthquake preparation zone. Besides, the vertical profile at the bottom of Lake Baikal is suitable for electromagnetic monitoring of the fault electrical resistivity changes. Altogether, the vertical voltage above the deep-water fault might be one of earthquake precursors.

**Key words** *Baikal rift zone – electromagnetic monitoring – transfer functions – resistivity changes of the fault*

## 1. Introduction

It is generally accepted that one of the possible precursors of earthquake in the seismically active Baikal region may be the change in the electrical resistivity of the saturated porous rock in deep-water rift faults. In accordance with the modern concept of the Baikal region geoelectrical structure (Merklin *et al.*, 1979), there is a narrow fault there that is galvanically connected with a deep-seated conductor. Berdichevsky *et al.* (1989) showed that for two-di-

mensional (2D) model of marine deep magnetotelluric investigations the vertical electric field at the ocean bottom is highly sensitive to the resistivity of the underlying cross-section. Besides, Berdichevsky *et al.* (1996) showed that certain 2D Earth models would generate considerable vertical electrical currents if the models include vertical faults of low resistivity. These authors used horizontal magnetotelluric field as an incident field. The latter work deals with magnetotellurics in the Lesser Caucasus but the first one deals with deep marine magnetotellurics. Meanwhile, Baikal water is fresh and much more resistive as compared with the oceanic water, however, Shneyer *et al.* (1998) proved that in 2D model of Southern Baikal the vertical electric field,  $E_z$ , is again sensitive to the presence of thin vertical fault of low resistivity. Though these results are valuable, we decided to explore the behaviour of  $E_z$  for a three-dimensional (3D) Baikal model, bearing in mind that the fault is a body of limited length but not of an infinite one. In this paper we build

---

*Mailing address:* Dr. Oleg V. Pankratov, Geoelectromagnetic Research Institute, Russian Academy of Sciences, 142190 Troitsk, P.O. Box 30, Moscow Region, Russia; e-mail: o.pankratov@mtu-net.ru

a simple 3D model of Southern Baikal and verify: 1) whether  $E_z$  is detectable over the fault, and 2) whether  $E_z$ -response is sensitive to the resistivity changes of the fault.

## 2. Model

Lake Baikal is located in the southern part of Eastern Siberia (see fig. 1). It is the oldest existing freshwater lake on Earth (20-25 million years old), being the deepest continental body of water.

It is 636 km long and 48 km wide. Baikal lies in a deep structural hollow surrounded by rock. The fault that we are interested in, is located at the southern part of Lake Baikal, not far from the town of Slydyanka. A simplified 3D resistivity model of the Baikal deep fault is shown in figs. 2 and 3. The geometry of the model was taken mainly from seismic data by Merklin *et al.* (1979), whereas the resistivity data were taken from electromagnetic data by Popov (1977), and Kieselev and Popov (1992). In the model the 2 km thick, 40  $\Omega\cdot\text{m}$  water layer is underlain by

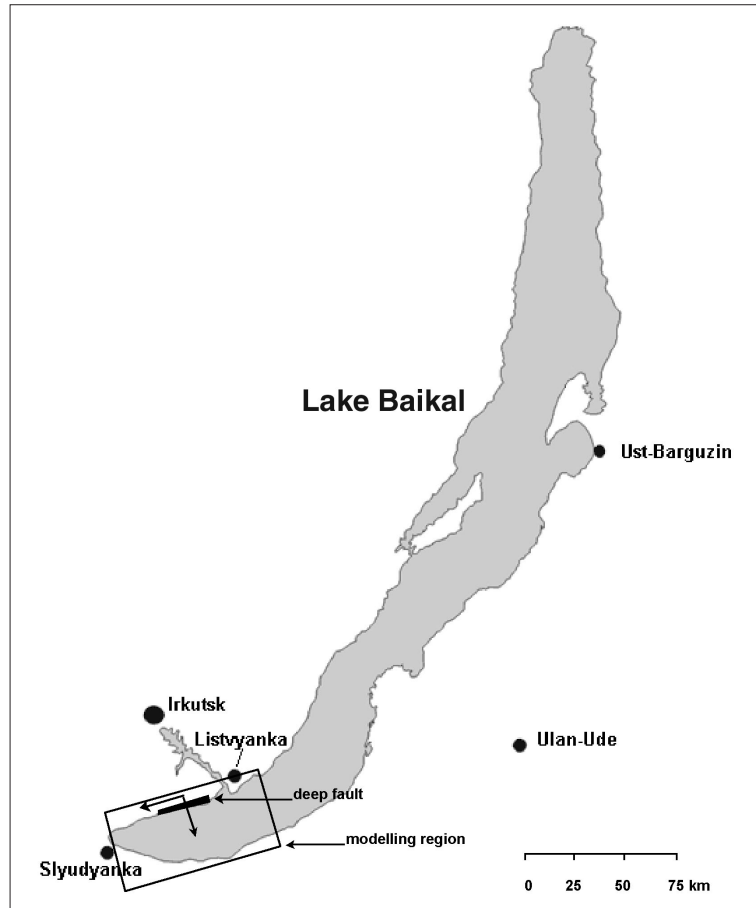


**Fig. 1.** Map of the region of Lake Baikal. Modelling region is marked with a rectangle. The fault is marked with a thick line.

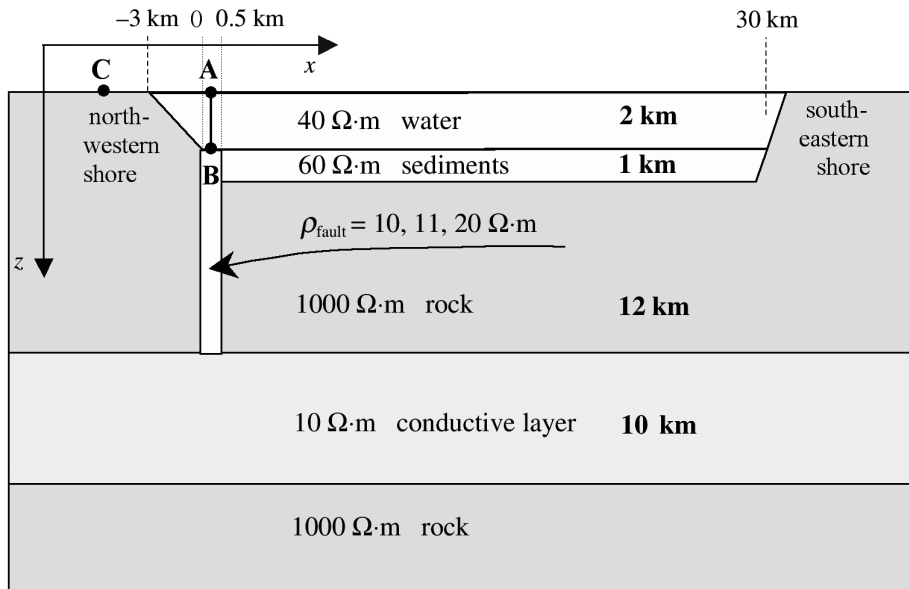


**Fig. 2.** 3D resistivity model of the Baikal Fault (side view). Line **A-B** is the profile where behaviour of  $E_z$  is studied. **C** is the coast site where components  $H_x$  and  $H_y$  are taken to obtain  $E_z$  response (see details in the text).

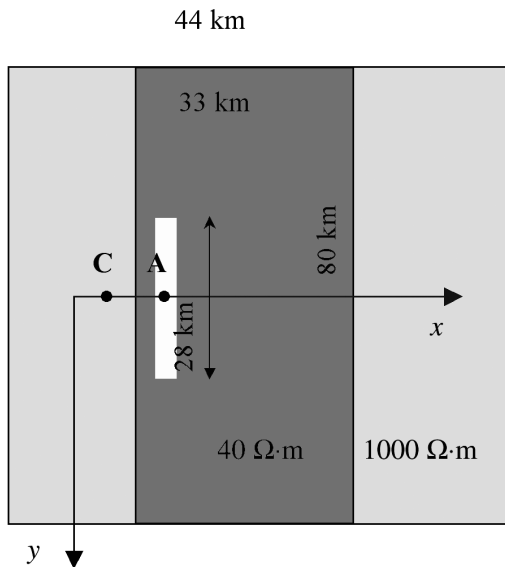


**Fig. 3.** 3D resistivity model (plane view).

the 1 km thick, 60  $\Omega\cdot\text{m}$  sedimentary layer. Both layers are surrounded and underlain by 1000  $\Omega\cdot\text{m}$  rock. Below, at a depth of 15 km, there is a 10 km thick conductive layer of 10  $\Omega\cdot\text{m}$ . As for the fault in the model, it is 28 km long in  $y$ -direction (parallel to the shore) and 0.5 km wide in  $x$ -direction (perpendicular to the shore). The vertical size of the fault is 13 km. The fault outcrop is located at lake bottom exactly where the 35° steep slope of the north-western shore of the lake is ending. The shape of the south-eastern shore slope has been proved not to affect the electromagnetic (EM) field calculated in the vicinity of north-western shore. Thus, the fault appears to be galvanically connecting the deep conductive layer under the lake and the lake itself.

### 3. Numerical modelling

In the 3D resistivity model proposed we have performed a series of simulations of the

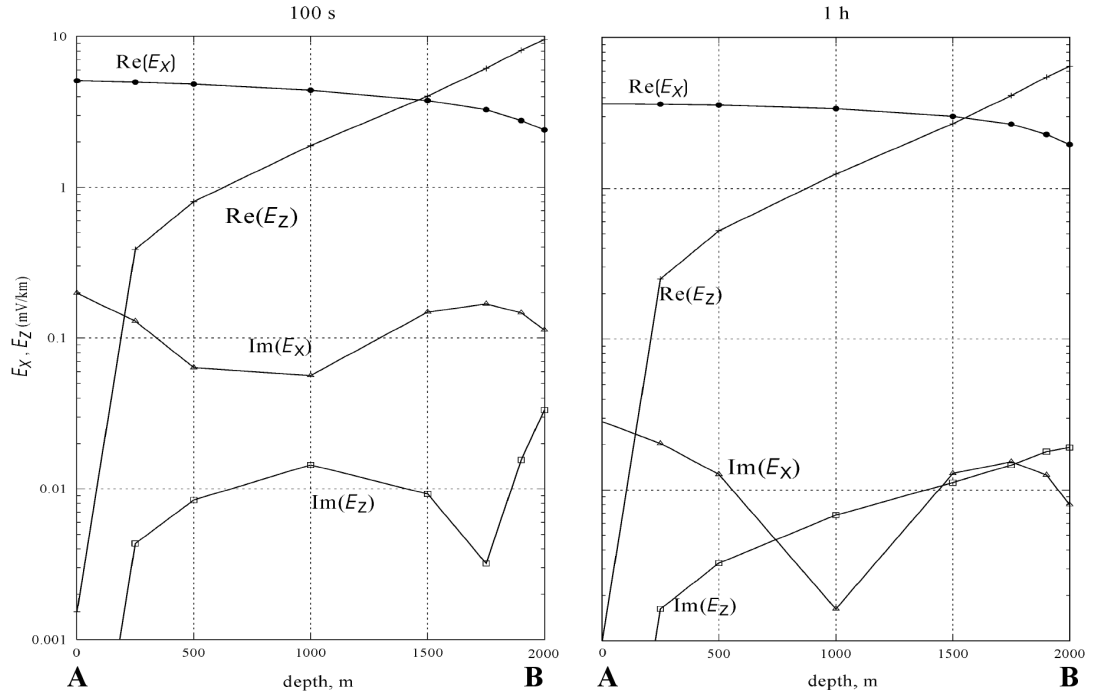
vertical electric field,  $E_z$ , along vertical profile **A-B** as well as horizontal magnetic field on the shore. This 2 km long profile (from lake surface to the bottom) is located just over the center of the fault (see fig. 2). The amplitude of the incident plane wave electric field is chosen to be equal to 10 mV/km, resembling typical amplitudes of mid-latitude disturbances. Period of the incident field is taken to be 100 s and 1 h. While modelling, we varied the fault resistivity,  $\rho_{\text{fault}}$ , the values taken to be 10, 11 and 20  $\Omega\cdot\text{m}$ . To perform the simulations we used X3D code which is based on the solution of modified scattering equation by the Krylov subspace iterations (Avdeev *et al.*, 1997, 2000). The modelling region of 44 km  $\times$  80 km  $\times$  15 km is divided into 440  $\times$  100  $\times$  14 cells.

Figure 4 presents the vertical electric field,  $E_z$ , along vertical profile **A-B** for  $E_x$ -polarized incident plane wave, with fault resistivity being

10  $\Omega\cdot\text{m}$ . Left and right panels of the figure reveal the results for the periods of 100 s and 1 h respectively. The figure demonstrates that the values of  $|E_z|$  are ranging, depending on depth, from zero (at the surface) up to 9 mV/km (at the bottom). In practice during the future experiment we are going to measure the vertical voltage,  $V(\mathbf{A}, \mathbf{B})$ , between points **A** and **B**. In our model,  $V(\mathbf{A}, \mathbf{B})$  can be calculated as

$$V(\mathbf{A}, \mathbf{B}) = \int_{\mathbf{A}}^{\mathbf{B}} E_z(z) dz..$$

The left plot in fig. 4 implies that the vertical voltage,  $V(\mathbf{A}, \mathbf{B})$ , should exceed 5 mV, which is very promising, since 5 mV could be readily detected by conventional EM instruments, their measurement precision accounting for 0.01 mV. In addition, it is also seen from the figure that



**Fig. 4.** Electric field components  $E_z$  and  $E_x$  along profile **A-B**. The source is  $E_x$ -polarized plane wave. The results are presented for periods 100 s (*left panel*) and for 1 h (*right panel*). The fault resistivity is 10  $\Omega\cdot\text{m}$ .

near the fault outcrop,  $E_z$ -field even dominates the primary field  $E_x$ . Note that only real parts of the components are discussed, since imaginary parts are two orders of magnitude less.

It can be seen from fig. 4  $E_z(z)$  that can be approximated as follows:

$$E_z(z) \approx E_z(b) e^{(z-b)/h} \quad (0 < z \leq b) \quad (3.1)$$

when we evaluate integral

$$V(\mathbf{A}, \mathbf{B}) = \int_{\mathbf{A}}^{\mathbf{B}} E_z(z) dz = \int_0^b E_z(z) dz.$$

Here  $b = 2$  km is the bottom depth. Also,  $h = 621$  m and  $h = 586$  m for period of 100 s and 1 h respectively. As a consequence, the vertical voltage is directly proportional to the vertical electric field measured at the bottom

$$V(\mathbf{A}, \mathbf{B}) = k \cdot E_z(b) \quad (3.2)$$

where proportionality coefficient is  $k = h(1 - e^{-b/h})$ . We can show that coefficient  $k$  does not depend on the amplitude of the incident field.

The other consequence: higher values of the vertical electric field are accumulated near the bottom, so that it is not necessary to locate point  $\mathbf{A}$  exactly at the surface. We can locate point  $\mathbf{A}$ , say, 100 or 200 m deeper without significant change in the value of  $V(\mathbf{A}, \mathbf{B})$ .

As for the other polarization of the incident field ( $E_y$ -polarized plane wave), the vertical electric field is at least two orders of magnitude less than that for  $E_x$ -polarized incident field.

So far we demonstrated the amplitudes of the fields themselves. But it is known that while monitoring, the external field should be excluded from consideration. For this purpose, we introduce  $E_z$ -response as the expansion coefficients in

$$V(\mathbf{A}, \mathbf{B}) = u_{zx} H_x^r + u_{zy} H_y^r \quad (3.3)$$

where  $H_x^r$  and  $H_y^r$  are the horizontal magnetic field components at the coastal reference site (site  $\mathbf{C}$ , see figs. 2 and 3).

Expansion (3.3) can be used in the following way. Let  $V^1(\mathbf{A}, \mathbf{B})$  and  $V^2(\mathbf{A}, \mathbf{B})$  be the vertical

voltage values measured for any two different polarizations of the incident field. Let  $(H_x^1, H_y^1)$  and  $(H_x^2, H_y^2)$  be the horizontal magnetic fields measured at the coastal reference site for the first and for the second polarization respectively. From expansion (3.3) it follows that:

$$\begin{aligned} V^1(\mathbf{A}, \mathbf{B}) &= u_{zx} H_x^1 + u_{zy} H_y^1 \\ V^2(\mathbf{A}, \mathbf{B}) &= u_{zx} H_x^2 + u_{zy} H_y^2. \end{aligned} \quad (3.4)$$

Therefore, we obtain final formulae for transfer functions  $u_{zx}$  and  $u_{zy}$  as follows

$$\begin{pmatrix} u_{zx} \\ u_{zy} \end{pmatrix} = \frac{1}{\det H} \begin{pmatrix} H_y^2 & -H_y^1 \\ -H_x^2 & H_x^1 \end{pmatrix} \begin{pmatrix} V^1(\mathbf{A}, \mathbf{B}) \\ V^2(\mathbf{A}, \mathbf{B}) \end{pmatrix} \quad (3.5)$$

where  $\det H = (H_x^1 H_x^2 - H_y^1 H_y^2)$ . Then these transfer functions  $u_{zx}$  and  $u_{zy}$  are called the  $E_z$ -responses because bigger values of the vertical electric field,  $E_z$ , are accumulated near the bottom and because  $V(\mathbf{A}, \mathbf{B})$  is proportional to  $E_z(b)$  (eq. (3.2)).

Table I presents the absolute value of the  $E_z$ -response,  $|u_{zy}|$ , shown with respect to the fault resistivity and period. Table I shows  $|u_{zy}|$  transfer function alone, since response  $u_{zx}$  appears to be negligibly small compared to  $u_{zy}$ . This is due to the fact that only TM-polarized incident field generates major vertical electrical current through the fault.

Although electromagnetic field components  $E_x$ ,  $E_y$ ,  $H_x$ ,  $H_y$ ,  $H_z$  appear to be insensitive to the

**Table I.** Absolute value of  $E_z$ -response,  $|u_{zy}|$ , with respect to the fault resistivity and period.

	$E_z$ -response (mV/nT)	
	100 s	1 h
$\rho_{\text{fault}} = 10 \Omega \cdot \text{m}$	$776 \cdot 10^{-9}$	$186 \cdot 10^{-9}$
$\rho_{\text{fault}} = 11 \Omega \cdot \text{m}$	$743 \cdot 10^{-9}$	$180 \cdot 10^{-9}$
$\rho_{\text{fault}} = 20 \Omega \cdot \text{m}$	$526 \cdot 10^{-9}$	$128 \cdot 10^{-9}$
precision of experimental $E_z$ -response	$14 \cdot 10^{-9}$	$5 \cdot 10^{-9}$

resistivity of the fault, we still need components  $H_x$  and  $H_y$  on the shore in order to obtain transfer functions  $u_{zx}$  and  $u_{zy}$ . Indeed, transfer functions  $u_{zx}$  and  $u_{zy}$  do not depend on the polarization of the incident field but the vertical voltage does.

The second row of table I shows that for a 100 s period, an operator should measure the values of 776, 743, and 526 and distinguish them from each other having the measurement precision equal to 14. Obviously it is possible. For a 1 h period, the measurement precision is just enough to distinguish the 10  $\Omega\cdot\text{m}$  fault from the 11  $\Omega\cdot\text{m}$  fault; and it is far enough to distinguish the 11  $\Omega\cdot\text{m}$  fault from the 20  $\Omega\cdot\text{m}$  fault. Altogether, for both periods the changes in the fault resistivity lead to detectable changes in  $E_z$ -responses. More explicitly, 10% and 100% fault resistivity changes result in 4% and 30%  $E_z$ -response changes, respectively. It should be also stressed that traditional impedance responses (simulated but not shown here) have appeared to be practically insensitive to the changes of the fault resistivity. Further numerical modelling (performed but not shown here) reveals that the link between the  $E_z$ -responses and the fault resistivity holds valid for bigger resistivity values. Namely, for the values  $\rho_{\text{fault}} = 10, 11, 12, 20, 40, 80, 160$  and  $320 \Omega\cdot\text{m}$  we calculated the  $E_z$ -responses and found that  $|u_{zy}(\rho_{\text{fault}})|$  can be approximated as follows:

$$|u_{zy}(\rho_{\text{fault}})| \approx \nu \cdot \rho_{\text{fault}}^\gamma \quad (3.6)$$

where  $\gamma = \gamma(T)$  and  $\nu = \nu(T)$  depend on the period,  $T$ , of the incident field. Approximation (3.6) now follows that though we could hardly distinguish the 10  $\Omega\cdot\text{m}$  fault from the 11  $\Omega\cdot\text{m}$  fault at 1 h period, the 10  $\Omega\cdot\text{m}$  fault can easily be distinguished from the 14  $\Omega\cdot\text{m}$  fault at this period.

Though our model is an estimate, we realize that the link between the  $E_z$ -responses and the fault resistivity is rough enough and it must be detected while *in situ* measurements.

#### 4. Conclusions

3D numerical studies have shown that the vertical voltage is detectable above the Baikal deep fault, and that  $E_z$ -responses are sensitive to

the resistivity changes of the fault, *i.e.*  $E_z$ -responses appear actually informative with respect to the resistivity «breath» of the fault. Further studies should include more detailed modelling and field operations. It should answer the question whether changes in  $E_z$ -responses (and  $\rho_{\text{fault}}$ ) are connected with changes in a stress state in the fault vicinity and whether  $E_z$ -responses can be used as one of earthquake precursors.

#### Acknowledgements

The research has been partly made possible through grants No. 00-05-64182 and No. 00-05-64677 from the Russian Foundation for Basic Research. We are also grateful for both reviewers' valuable comments.

#### REFERENCES

- AVDEEV, D.B., A.V. KUVSHINOV, O.V. PANKRATOV and G.A. NEWMAN (1997): High performance three-dimensional electromagnetic modelling using modified Neumann series. Wide-band numerical solution and examples, *J. Geomag. Geoelectr.*, **49**, 1519-1539.
- AVDEEV, D.B., A.V. KUVSHINOV, O.V. PANKRATOV and G.A. NEWMAN (2000): 3D EM modelling using fast integral equation approach with Krylov subspace accelerator, in *Extended Abstracts of the 62nd Meeting of European Association of Geoscientist and Engineers*, vol. 2, p. 183.
- BERDICHEVSKY, M.N., O.N. ZHDANOVA and M.S. ZHDANOV (1989): *Marine Deep Geoelectricity* (Nauka, Moscow), pp. 90.
- BERDICHEVSKY, M.N., V.P. BORISOVA, N.S. GOLUBTSOVA, A.I. INGEROV, YU.F. KONOVALOV, A.V. KULIKOV, L.N. SOLODILOV, G.A. CHERNYAVSKY and I.P. SHPAK (1996): An experience of interpretation of MT soundings in the Lesser Caucasus mountains, *Fiz. Zemli*, **4**, 99-117 (in Russian).
- KIESELEV, A.I. and A.M. POPOV (1992): Asthenospheric diapir beneath the Baikal rift: petrological constraints, *Tectonophysics*, **208**, 287-295.
- MERKLIN, L.R., V.E. MILANOVSKIY, V.I. GALKIN and M.V. ZAKHAROV (1979): Structure of sedimentary layer and basement relief, in *Gelologic-Hydrophysical and Deep-Water Studies at Lake Baikal*, 104-110.
- POPOV, A.M. (1977): High conductive deep layers as they found from magnetotelluric data, in *Deep Structure of the Baikal Rift* (Nauka, Novosibirsk), (in Russian).
- SHNEYER, V.S., E.YU. SOKOLOVA and I.L. TROFIMOV (1998): Two-dimensional electromagnetic field modelling results in the South-Baikal depression region, in *Abstract of 4th International Conference: Modern Methods and Techniques of Oceanological Research*, Moscow (in Russian).